

This article was downloaded by:

On: 27 January 2011

Access details: *Access Details: Free Access*

Publisher *Taylor & Francis*

Informa Ltd Registered in England and Wales Registered Number: 1072954 Registered office: Mortimer House, 37-41 Mortimer Street, London W1T 3JH, UK



Phosphorus, Sulfur, and Silicon and the Related Elements

Publication details, including instructions for authors and subscription information:

<http://www.informaworld.com/smpp/title~content=t713618290>

The Design of Multifunctional Antioxidants Against the Damaging Ingredients of Oxidative Stress

Susanne Mecklenburg^a; Catriona A. Collins^b; Mandy Döring^a; Torsten Burkholz^a; Muhammad Abbas^a; Fiona H. Fry^b; Charareh Pourzand^c; Claus Jacob^a

^a Division of Bioorganic Chemistry, School of Pharmacy, Saarland University, Saarbruecken, Germany

^b School of Biosciences, University of Exeter, Exeter, United Kingdom ^c Department of Pharmacy and Pharmacology, University of Bath, Claverton Down, Bath, United Kingdom

To cite this Article Mecklenburg, Susanne , Collins, Catriona A. , Döring, Mandy , Burkholz, Torsten , Abbas, Muhammad , Fry, Fiona H. , Pourzand, Charareh and Jacob, Claus(2008) 'The Design of Multifunctional Antioxidants Against the Damaging Ingredients of Oxidative Stress', *Phosphorus, Sulfur, and Silicon and the Related Elements*, 183: 4, 863 — 888

To link to this Article: DOI: 10.1080/10426500801898200

URL: <http://dx.doi.org/10.1080/10426500801898200>

PLEASE SCROLL DOWN FOR ARTICLE

Full terms and conditions of use: <http://www.informaworld.com/terms-and-conditions-of-access.pdf>

This article may be used for research, teaching and private study purposes. Any substantial or systematic reproduction, re-distribution, re-selling, loan or sub-licensing, systematic supply or distribution in any form to anyone is expressly forbidden.

The publisher does not give any warranty express or implied or make any representation that the contents will be complete or accurate or up to date. The accuracy of any instructions, formulae and drug doses should be independently verified with primary sources. The publisher shall not be liable for any loss, actions, claims, proceedings, demand or costs or damages whatsoever or howsoever caused arising directly or indirectly in connection with or arising out of the use of this material.

The Design of Multifunctional Antioxidants Against the Damaging Ingredients of Oxidative Stress

Susanne Mecklenburg,¹ Catriona A. Collins,²
Mandy Döring,¹ Torsten Burkholz,¹ Muhammad Abbas,¹
Fiona H. Fry,² Charareh Pourzand,³ and Claus Jacob¹

¹Division of Bioorganic Chemistry, School of Pharmacy, Saarland University, D-66041 Saarbruecken, Germany

²School of Biosciences, University of Exeter, Exeter EX4 4 QD, United Kingdom

³Department of Pharmacy and Pharmacology, University of Bath, Claverton Down, Bath BA2 7AY, United Kingdom

Oxidative stress is a biochemical condition associated with a sharp increase in intracellular concentrations of a range of oxidative stressors, including reactive oxygen species, reactive nitrogen species and labile metal ions. It is associated with a wide range of human disorders, such as inflammatory diseases, neurodegenerative diseases, glaucoma, and cancer. Equally importantly, oxidative stress is pronounced in older people, which makes it an important matter in an ageing Society. Not surprisingly, antioxidants have become a major focus of modern drug development. While natural antioxidants, such as phenolic aromatic compounds, vitamin C, vitamin E and curcumin have shown promising results, the development of effective synthetic antioxidants is often problematic. We have recently proposed the rational design of multifunctional antioxidants which target oxidative stressors in a more comprehensive manner. Such compounds may, for instance, combine catalytic sites with metal binding sites. Here we present the synthesis of representative molecules with combined catalytic and metal binding properties. The apparent 'antioxidant'

The authors are indebted to the following colleagues in the UK and Germany for their tireless support and advice with synthesis, electrochemistry, complex chemistry and, of course, working with FEK4 and FCP7 cells: Rex Tyrrell (University of Bath), Jennifer Littlechild (University of Exeter), James Tucker (University of Birmingham), Kaspar Hegetschweiler (Saarland University) and Awais Anwar (Saarland University).

The authors would also like to acknowledge financial support from Saarland University, the Ministry of Culture of the Saarland, Fresenius Medical Care (stipend T.B.), DAART (UK) (stipend for C.A.C.), EATL (for F.H.F.) and the University of Exeter. This financial support has not caused any conflict of interest to any of the participating authors.

Address correspondence to Claus Jacob, Division of Bioorganic Chemistry, School of Pharmacy, Universitaet des Saarlandes, Campus B 2.1, P O Box 151150 D-66041, Saarbruecken, Germany. E-mail: c.jacob@mx.uni-saarland.de

activities have been studied in vitro and, for the most promising compound, have been confirmed in cultured skin cells exposed to UVA radiation.

Keywords Antioxidants; catalysis; metal binding; radiation damage; selenium

INTRODUCTION

Oxidative stress (OS) is a biochemical condition associated with a significant increase of oxidative stressors, such as reactive oxygen species (ROS), peroxynitrite and free radicals.¹ It can have various causes, among them an impaired antioxidant cellular defense, and manifests itself in a range of human disorders. The latter may, for instance, include various auto-inflammatory diseases, Rheumatoid Arthritis, neurodegenerative diseases (including Alzheimer's disease and Parkinson's disease), glaucoma, diabetes, and cancer.

Importantly, OS is not only a hallmark of many human illnesses, but also occurs in humans as part of the normal ageing process.¹ Although OS does not immediately cause illnesses in older people, it nonetheless poses a certain kind of "burden" for them. It may, for instance, ultimately lead to various disorders associated with OS, most notably perhaps inflammatory diseases and cancer. As a result, OS has become an important center point of research into the causes and possible treatments of OS-related diseases.

While OS itself is seldom the ultimate cause of these diseases, it can be seen as a point of intervention, either preventive or therapeutically. Within this context, antioxidants provide a certain protection from OS. Research in this group of compounds has increased dramatically during the last decade, and antioxidants such as vitamin C, α -tocopherol, curcumin and various natural phenolic aromatic compounds (e.g., catechins, quercetin derivatives), have been associated with disease preventive and possibly therapeutic properties.

Among the most interesting antioxidants are catalytic antioxidants, such as the antioxidant enzymes superoxide dismutase (Cu,Zn-SOD and Mn-SOD), catalase (CAT), glutathione peroxidase (GPx) and peroxiredoxins (Prx).^{1,2} Compared to simple reducing agents, such as glutathione (GSH), these natural catalysts have several significant advantages. First, they react rapidly with oxidative stressors, such as the superoxide radical anion and H_2O_2 . In many cases, the rate constants of these catalytic reactions are orders of magnitude higher than the ones of un-catalyzed interactions, e.g., the reduction of H_2O_2 by GSH takes hours in the absence of GPx, and seconds in its presence. Secondly, the "chemistry" of these catalysts is tightly controlled, i.e., they produce harmless side-products when compared to some of the reaction

products of other antioxidants. And, perhaps most importantly, catalysts are recycled, and at minute concentrations can perform the same ROS reduction reaction thousands of times, compared to just once by one-shot antioxidants, which need to react in stoichiometric amounts.³

Not surprisingly, the development of synthetic antioxidants, which mimic the catalytic activity of these enzymes, has recently been at the forefront of antioxidant development. Among the antioxidant enzymes in question, the selenium enzyme GPx provides a particularly interesting template for mimics.⁴ Selenium (and tellurium) compounds are more stable chemically and metabolically when compared to metal-complexes mimicking the SOD and CAT enzymes. At the same time, comparably simple Se compounds are able to catalyze the reaction of H_2O_2 with GSH to H_2O and GSSG effectively. In contrast, potential Prx-mimics are more difficult to devise, since the catalytic sulfur in these enzymes forms a transient sulfenic acid (RSOH), which is fine in the active site of the enzymes, but too reactive in most small molecules, where it readily reacts with thiols to form a disulfide and water.

Nonetheless, the notion that one antioxidant enzyme mimic alone may mount an effective antioxidant defense is hampered by the fact that OS is a multi-stressor event.¹ By simply targeting one of the many oxidative stressors, other stress events will largely go unaffected and continue to damage the cell. We have therefore recently proposed the use of multifunctional antioxidants to impair oxidative stressors more widely (Figure 1).⁵ At the time, two oxidative stressors, H_2O_2 and labile, redox active metal ions, such as $\text{Cu}^{+/2+}$ and $\text{Fe}^{2+/3+}$ were chosen as possible targets. Both stressors form key junctions at OS redox cascades: H_2O_2 is the follow-on product of $\text{O}_2^{\bullet-}$ and a direct precursor of the highly reactive hydroxyl radical (HO^\bullet). It is also a substrate of myeloperoxidase and hence a precursor of hypochlorous acid, HOCl . Labile copper and iron ions, which may have been liberated from proteins by ROS, catalyze the reduction of H_2O_2 to HO^\bullet in Fenton-type reactions. Hydroxyl radicals, in turn, may attack metalloproteins and liberate more copper and iron ions, entering a vicious, oxidizing cycle involving H_2O_2 and copper/iron ions.¹

As part of our previous studies, selenium derivatives of pyridine, aniline and quinoline, i.e., 2,2'-diselane-1,2-diylpyridine, 2,2'-diselane-1,2-diylaniline, 8,8'-diselane-1,2-diylquinoline, respectively, were synthesized (Figure 2).⁵ These compounds were chosen as representatives of different classes of nitrogen/selenium compounds which may bind metals via the N and Se atom. They were subsequently evaluated for catalytic, metal binding and antioxidant activity in a range of in vitro assays and fibroblast (FEK4 and FCP7) cell culture. In essence, 2,2'-diselane-1,2-diylaniline exhibited the best protection against cell

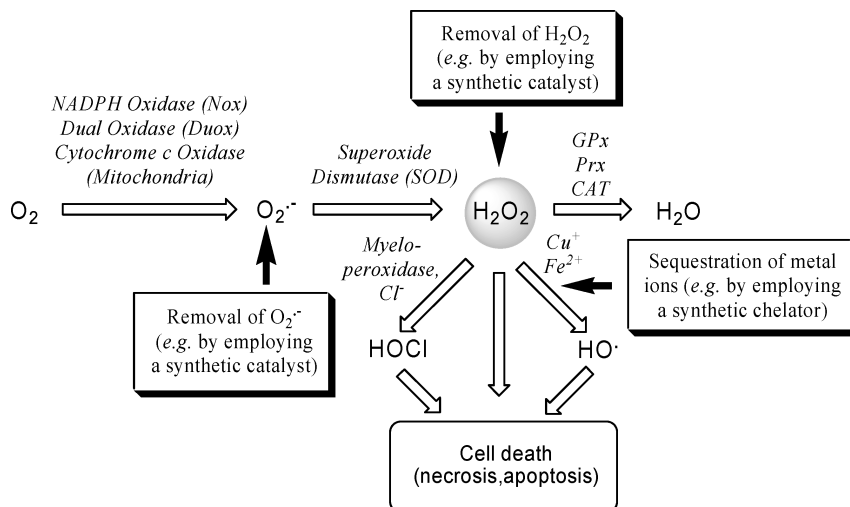


FIGURE 1 The cascade of reactive oxygen species (ROS) leading to cell damage and cell death. This cascade of ROS offers several points of intervention, among them catalysts with SOD-like and GPx-like activity and removal of labile copper and iron ions to prevent HO^\bullet formation. Together, these points of intervention provide the basis for the design of multifunctional agents discussed here. Other approaches, such as inhibition of SOD by 2-methoxyestradiol or inhibition of myeloperoxidase, have also been discussed in the literature, yet are not free of possible complications (such as $O_2^{\bullet -}$ or H_2O_2 build-up, respectively).^{1,31} Inhibitions of Nox and Duox are also possible. Please note that this sketch of biochemical processes is necessarily incomplete. Reduction of H_2O_2 to HO^\bullet by metal ions may be catalytic in the presence of intracellular reducing agents.

damage induced by UVA-radiation.⁵ This compound was more active in this cell culture model when compared to the benchmark catalytic antioxidant ebselen. It also exhibited a comparably low electrochemical potential and interacted with Cu^{2+} ions, as shown by Differential Pulse Polarography and UV/VIS spectrophotometry.

Nonetheless, this compound primarily exerted its effects in the fibroblast cells by raising the total level of GPx-like activity. In contrast, there was little evidence of interaction with the labile iron pool, as measured by using the Calcein loading assay. In this respect, the weakly coordinating nitrogen/selenium-ligands were obviously inferior to the classical metal chelator, desferrioxamine (DFO), which is currently used to treat metal-related aspects of OS. In turn, the employment of considerably higher concentrations of Se-compounds, which may ultimately affect the labile iron pool, was unrealistic.

In order to address this apparent problem, a set of new compounds has now been chosen to combine GPx-like catalytic activity

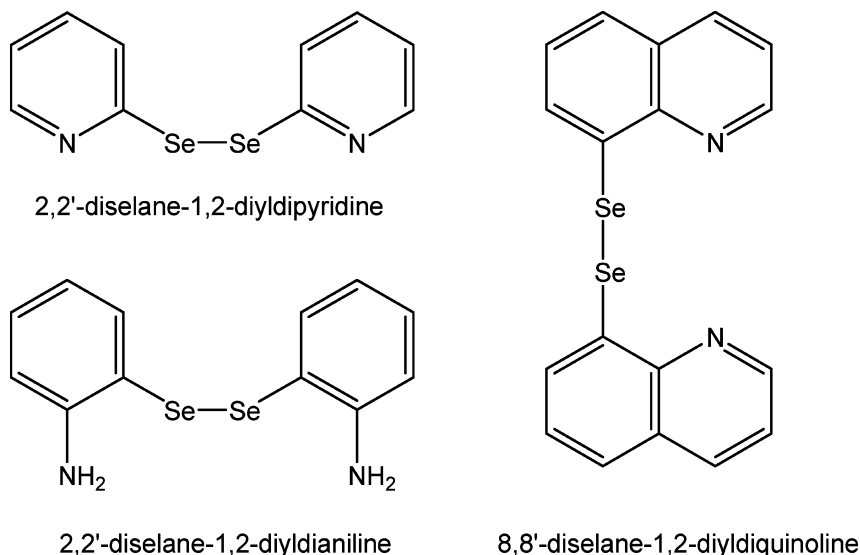


FIGURE 2 Multifunctional agents tested previously. While 2,2'-diselane-1,2-diyl dianiline, and to a lesser extent 2,2'-diselane-1,2-diylpyridine, protect cultured FCP7 fibroblast cells against UVA radiation, 8,8'-diselane-1,2-diylquinoline acts as photosensitizer.⁵ Mechanistic studies in cell culture indicate that the protective effect associated with these compounds is mostly the result of GPx-like activity.

with enhanced metal binding properties. Here, we briefly describe the synthesis of three representative compounds, their electrochemical behavior, and interaction with metal ions. We also demonstrate a rather promising antioxidant activity for one of the compounds in cultured FEK4 cells under UVA radiation-induced OS.

RESULTS

Figure 3 shows the three multifunctional compounds (**1–3**) selected for this study. These compounds were chosen because they combine a catalytic Se atom with a metal binding site. The catalytic site is similar to the one found in other, conventional GPx-mimics, with selenium attached to one aromatic residue for increased chemical and metabolic stability. The metal binding sites of these compounds are based on well-known copper/iron binding sites, i.e., tacn (1,4,7-triazacyclononane), cyclen (1,4,7,10-tetraazacyclododecane) and protoporphyrin IX. The latter is particularly interesting, since it not only lends itself to the sequestration of adventitious metal ions, but may also provide the precursor

for metalloporphyrins and their associated, often catalytic activity (e.g. as SOD-mimics).^{6–8}

Synthesis of Compounds

Compounds **1–3** were synthesized successfully, albeit at rather modest yields. The individual synthetic pathways are shown in Figure 3a to Figure 3c. All three compounds were not previously reported in the literature. Analytical data obtained for these compounds, such as ¹H NMR, ¹³C NMR and LC-MS confirmed the structures proposed, whilst HPLC ascertained the purity of the compounds required for biochemical and cell culture studies. Within this context, the synthesis of compounds **1** and **2** was based on the coupling of a selenium-containing precursor on the well-known macrocycles tacn and cyclen. In case of **2**, two alternative avenues were followed (Figure 3b), both of which resulted in the desired product at comparable yields. In contrast, the synthesis of **3** was based on rather straightforward acid/amine coupling procedures between protoporphyrin IX and the Se-containing amine precursor (Figure 3c). The two coupling methods employed both led to the formation of **3**—with the ethylchloroformate method the milder and in the end more promising avenue.

Interaction of Compounds with Metal Ions

Interactions with metal ions (Cu²⁺, Fe²⁺, Fe³⁺, and Zn²⁺) were evaluated using Cyclic Voltammetry (for **1** and **2**), and because of appropriate spectroscopic properties, with UV/VIS spectrophotometry (for **3**).

Cyclic Voltammetry was used to investigate the influence of compounds on the redox behavior of Cu²⁺ ions, which are particularly

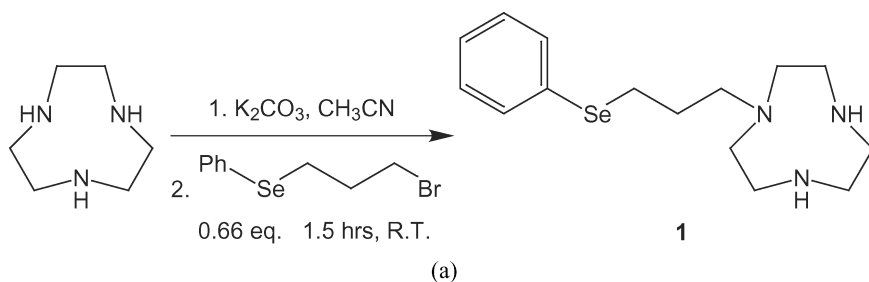


FIGURE 3 Synthesis of compounds **1–3**. Details of the synthetic pathways are provided in the text. The sulfur analogue of **3** was synthesized according to the same method. (*Continued*)

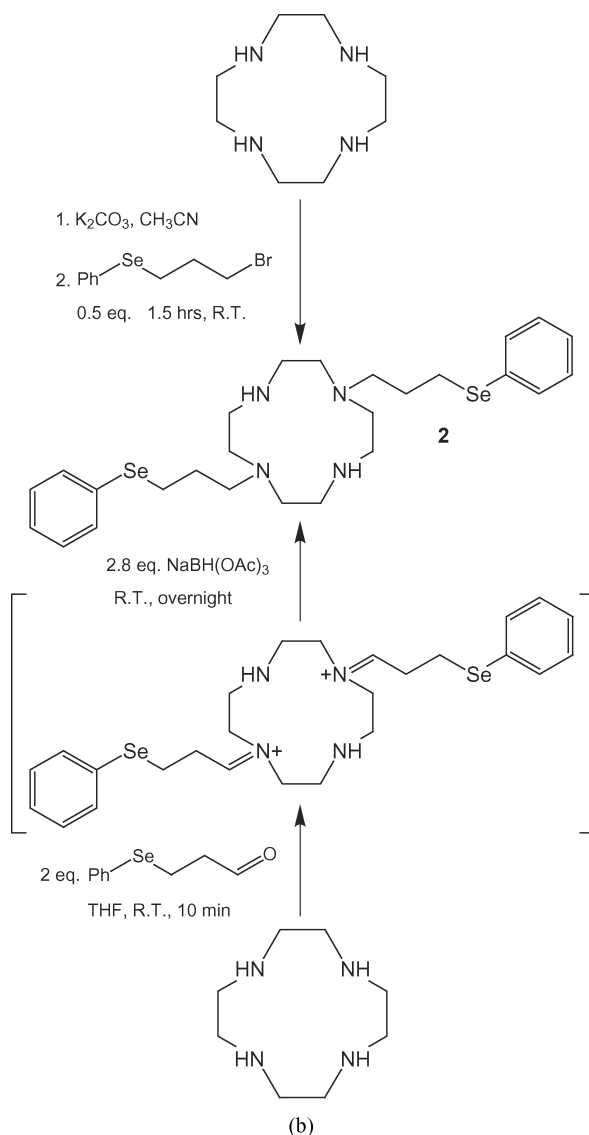


FIGURE 3 Continued

damaging when acting as Fenton-type catalysts during OS. Figure 4 illustrates the interactions of **1** and **2** with Cu^{2+} ions. Under the experimental conditions chosen, the copper ion exhibits a reduction peak at $E_{\text{pc}} = -180$ mV and an oxidation signal $E_{\text{pa}} = +330$ mV vs. the Ag/AgCl reference electrode (SSE). The one electron transfer between

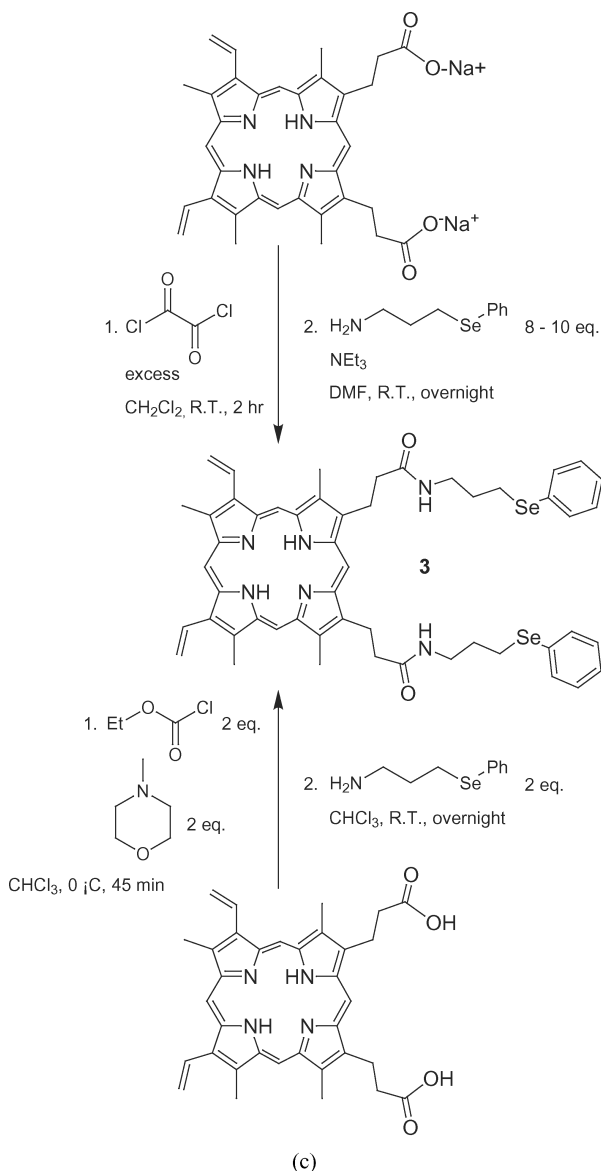
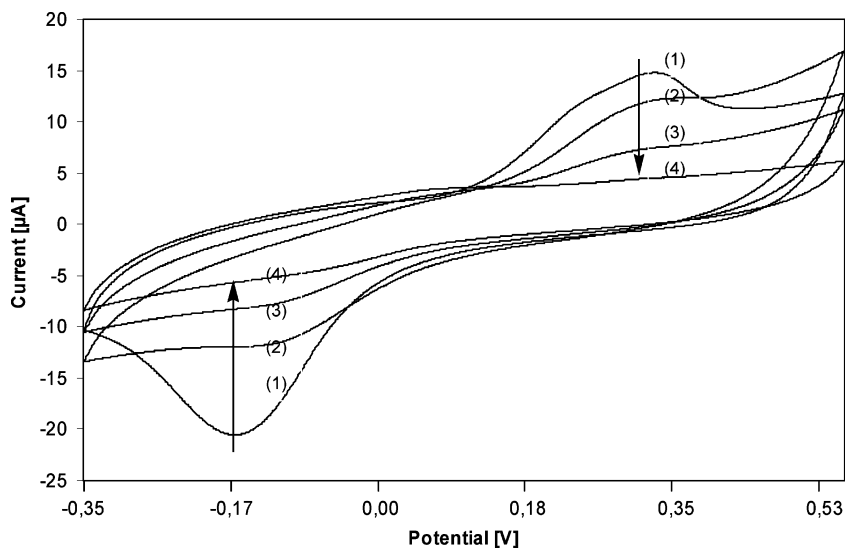
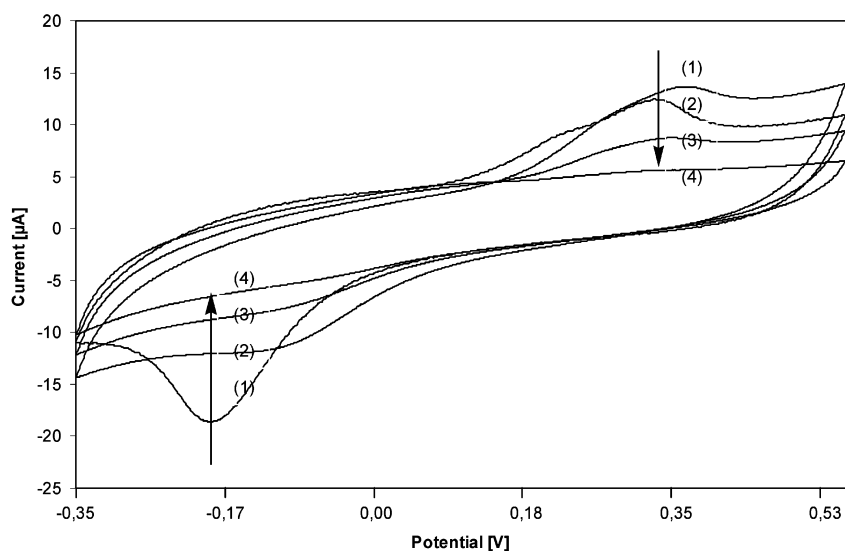


FIGURE 3 Continued

Cu^{2+} and Cu^+ is quasi-reversible ($\Delta E = 510$ mV), with a formal redox potential of $E^{0'} = +75$ mV. Addition of **1** and **2** results in a depression of both, the oxidation and reduction signal of the copper ion, which disappear at a ligand to metal ratio of approximately 1:1 (Figure 4a



(a)



(b)

FIGURE 4 Electrochemical changes of copper oxidation/reduction upon addition of **1** and **2** (Figure 4a and 4b, respectively). The addition of both compounds resulted in a significant decrease of peak currents. Ratios of compound to Cu^{2+} were 0, 0.33, 0.5 and 1.0 for (1) to (4). Experimental details are given in the text. Similar results were also obtained when DFO was used. A similar effect was observed for the electrochemical behavior of iron ions.

for **1**, Figure 4b for **2**). There were also slight shifts in E_{pa} and E_{pc} upon addition of ligand, but these changes were within the margins of experimental error. In order to confirm that metal binding effects were responsible for the disappearance of the reduction and oxidation waves, DFO was used as a positive control. This compound also led to a complete depression of the oxidation and reduction peaks of the Cu^{2+}/Cu^{+} redox pair. Similar results were obtained with ironions: The reduction peak of Fe^{3+} , which was observable under the conditions used at $E_{pa} = -400$ mV, decreased significantly upon addition of **1**, **2** and DFO.⁹

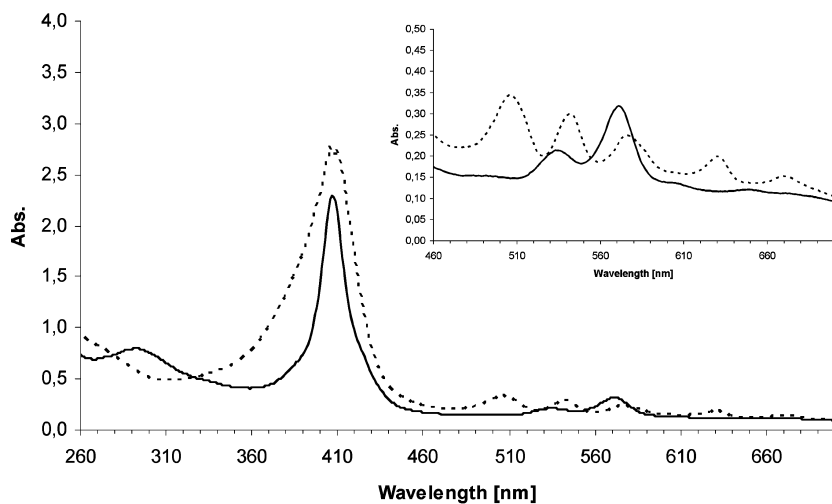
While compound **3** was too insoluble to be used in electrochemical experiments (concentrations of around 100 μM are required to produce reliable results by Cyclic Voltammetry), its spectrophotometric properties could be used to assess metal binding and exchange.

As expected, the protoporphyrin-containing molecule was able to interact with copper, iron and zinc ions. Binding of Cu^{2+} , Fe^{2+} , and Fe^{3+} resulted in significant changes to the compound's UV/VIS absorption spectrum, especially in the region between 450 and 700 nm (Figure 5). Importantly, all metals were added as chlorides, hence ruling out any specific effects due to different counter anions, such as ligand binding.

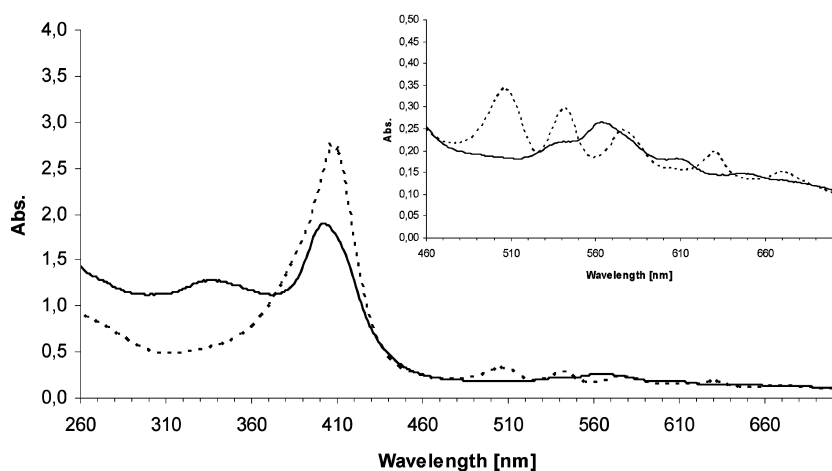
In short, addition of Cu^{2+} resulted in a decrease of absorbance bands at 407 nm (Soret band), 504, 541, 576, 628, and 669 nm. In turn, there were distinct signals for the copper complex at 532, 569, and 602 nm (Figure 5a).¹⁰ The interaction with Fe^{2+} resulted in a slight shift and decrease of the Soret band from 407 nm to 400 nm. As for copper, the smaller bands at 504, 541, 576, 628, and 669 nm all decreased (or were shifted) with new transitions at 535, 561, and 608 nm. Addition of Fe^{3+} slightly decreased and shifted the Soret band to 411 nm, resulted in the characteristic decreases/shifts of absorbancies between 500 and 700 nm and, like Fe^{2+} , led to characteristic signals at 535, 560, and 606 nm. In contrast, Zn^{2+} ions, which are known to bind strongly to protoporphyrin IX, had only a marginal effect on the electronic spectrum of **3** with a slight decrease and shift in the Soret band from 407 to 411 nm.

Similar results were obtained for protoporphyrin IX itself, which was used as a control and to find out if modification of the protoporphyrin with the Se-moiety causes any significant changes in the macrocycle's behavior toward metal ions. The similarity of results for **3**, its protoporphyrin precursor, and its sulfur-analogue (which was tested alongside **3**) indicates that this is clearly not the case.

Since there were significant differences between the spectra of **3** in the presence of copper and iron on the one hand, and zinc on the other, it was possible to qualitatively ascertain metal preferences of **3**. The behavior of the metal-loaded forms of **3** in the presence of equimolar



(a)



(b)

FIGURE 5 Interaction of **3** with metal ions as monitored by UV/VIS spectrophotometry. Spectra were recorded in CHCl_3 at 20°C for biochemically relevant Cu^{2+} , Fe^{2+} , Fe^{3+} and Zn^{2+} ions and are shown for Cu^{2+} and Fe^{2+} (Figure 5a and 5b, respectively). The absorption spectrum of **3** ($10\ \mu\text{M}$) is shown as broken lines (---) before and as solid lines (—) after addition of metal ions ($100\ \mu\text{M}$). Addition of Cu^{2+} and Fe^{2+} ions (as CuCl_2 and FeCl_2 in methanol, respectively) resulted in significant changes in the spectrum, which are detailed in the text. The addition of $100\ \mu\text{M}$ Fe^{3+} (as FeCl_3) resulted in changes almost identical to the ones observed for Fe^{2+} . Addition of Zn^{2+} (as ZnCl_2) did not alter the spectrum of **3** significantly.

amounts and 3-fold excess of other metals was therefore monitored. The behavior of Cu^{2+} and $\text{Fe}^{2+}/\text{Fe}^{3+}$ in the presence of Zn^{2+} was of particular interest: Is **3** able to uptake a redox-active, damaging metal ion (copper or iron) and simultaneous release/ignore a more benign, antioxidant metal (zinc)?

In short, addition of equimolar amounts or a 3-fold excess of Cu^{2+} , Fe^{2+} , and Fe^{3+} over Zn^{2+} to the zinc-form of **3** resulted in spectra characteristic of the Cu^{2+} , Fe^{2+} and Fe^{3+} forms of **3**, while addition of equimolar amounts or a 3-fold excess of Zn^{2+} over Cu^{2+} or Fe^{2+} to the copper- or iron-form of **3** did not change the spectra characteristic of the copper- or iron complex. The results for Cu^{2+} and Fe^{2+} are shown in Figure 6. Taken together, they indicate that Cu^{2+} and Fe^{2+} ions are indeed taken up by **3** in the presence of Zn^{2+} , an effect also observed for Fe^{3+} (spectrum not shown). Please note that these results are of a qualitative nature, performed in an organic solvent and clearly must be followed by a full complexometric study in the future.

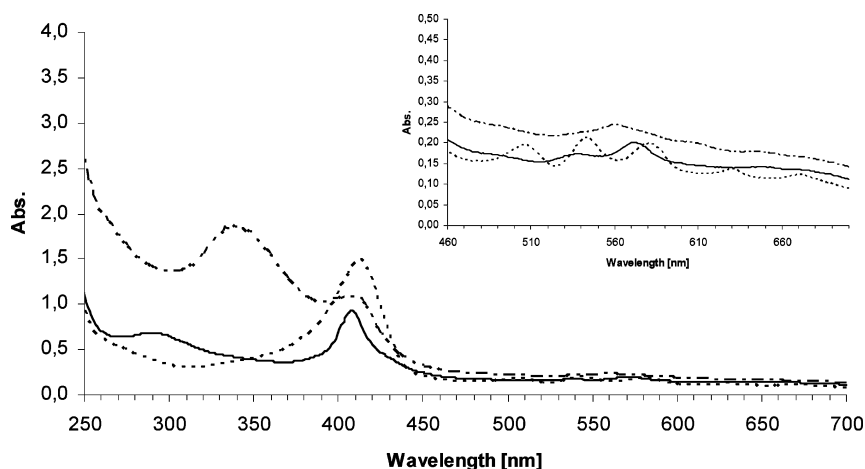


FIGURE 6 Metal exchange at the metal binding site of **3**. Spectra were recorded as described for Figure 5. The zinc complex (broken lines (---)) was formed by addition of 100 μM ZnCl_2 to 10 μM of **3**. Addition of 300 μM Cu^{2+} or Fe^{2+} resulted in spectral changes indicative of the formation of the Cu^{2+} and Fe^{2+} complex (solid (—) and dotted line (•—•—•), respectively). The same changes were observed for 100 μM Cu^{2+} or Fe^{2+} . This qualitative experiment demonstrates that Cu^{2+} and Fe^{2+} are able to compete with/substitute for Zn^{2+} . The resulting “copper (iron) for zinc” behavior has significant biochemical implications as described in the text.

The Catalytic Site

The redox properties of **1–3** were investigated using electrochemistry (Cyclic Voltammetry), the thiophenol (PhSH) and the metallothionein (MT) assays.^{5,11} Cyclic Voltammetry provides initial information about oxidation and reduction processes associated with the selenium atom, such as the position of the oxidation peak *E*_{pa}. The PhSH assay is indicative of the reaction of H₂O₂ with GSH. The MT assay measures zinc release from this zinc-sulfur protein in the presence of a peroxide, namely ^tBuOOH.

Compounds **1** and **2** exhibited a Se-oxidation peak (*E*_{pa}) at around +1200 mV vs. SSE. The lack of a corresponding reduction signal is evidence of an irreversible oxidation of the Se-atom to a selenium cation, which reacts further in aqueous solution. The *E*_{pa} values for **1** and **2** are rather positive and point towards electrochemically active, but not particularly reducing selenium-compounds.¹²

The rather modest 'activity' of the selenium redox center was confirmed in the PhSH and MT assays.⁵ In the PhSH assay, **1–3** only slightly enhanced the rate of PhSH oxidation in the presence of H₂O₂ (1.9-fold increase by **1**, 2.5-fold by **2**, approx. 1.1-fold increase by **3** from 8 nMs⁻¹ for the non-catalyzed reaction, respectively). Compound **1** was also tested in the MT assay, where it enhanced zinc release from MT in the presence of ^tBuOOH within 60 min from 15 to 23%. In comparison, selenols tested previously led to rates of up to 600 nMs⁻¹ in the PhSH assay and almost 80% zinc release in the MT assay.

The in vitro studies identified **1** and **2** as the more promising compounds, i.e., as (modest) reducing agents/GPx-like catalysts with good metal binding properties and a reasonable solubility in aqueous media. The efficiency of **3** remained somewhat vague due to low solubility in aqueous media. Since tacn has previously been associated with antioxidant activity, it was decided to test **1** in FEK4 fibroblast cell culture initially.

Antioxidant Activity in Fibroblast Cell Culture

In order to determine the antioxidant capacity of **1**, FEK4 cells were grown and exposed to 500 kJ m⁻² UVA radiation for 18 h in the absence and presence of **1** and tacn as Se-free control.¹³ The subsequently performed MTT (3-(4,5-dimethylthiazol-2-yl)-2,5-diphenyltetrazolium bromide) cell survival assay indicates that 50 μM of **1** is able to prevent virtually all OS damage caused by UVA radiation, while tacn itself is only modestly active at this concentration (Figure 7). Importantly, neither tacn nor **1** were themselves cytotoxic at the concentrations

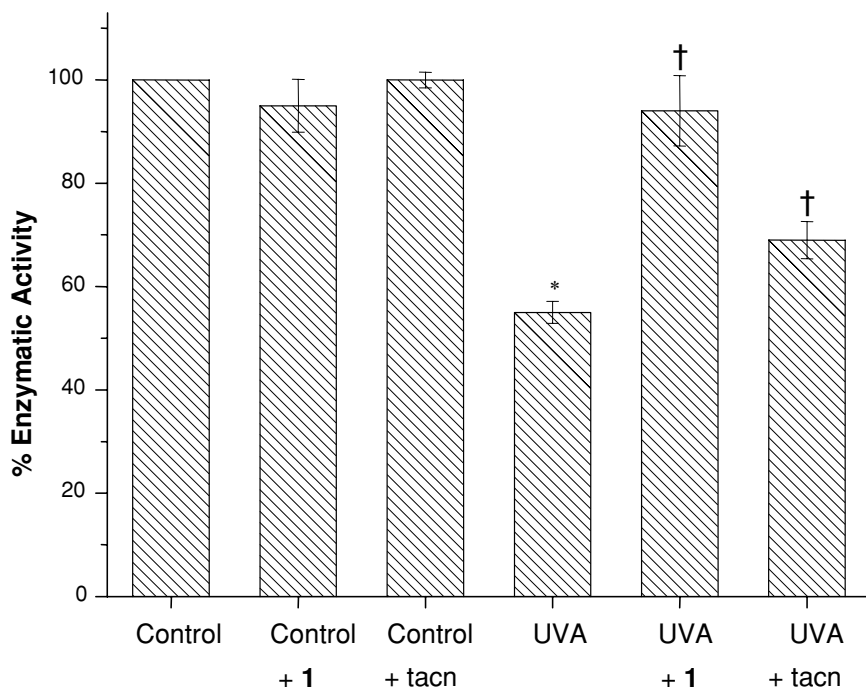


FIGURE 7 Protective effects of **1** (50 μM) on FEK4 fibroblast cells exposed to 500 kJm^{-2} UVA radiation. Cells were incubated with **1** or tacn 18 h previous to exposure. Cell viability was determined 4 h after irradiation using the standard MTT assay.^{5,13,14} Tacn (50 μM), which reflects the metal binding chemistry of **1**, was used for comparison. Data are means \pm SD of 3 samples from 3 independent experiments. *Significantly different from non-irradiated control; †Significantly different from UVA-irradiated control, $P < 0.05$.

used. Indeed, separate studies measuring the cytotoxicity of compounds confirmed that **1** was non-toxic (i.e., cell viability $> 90\%$) in FEK4 cells up to 100 μM , while the benchmark compound ebselen already showed toxic effects at 15 μM concentrations (measured in FCP7).

In order to find out if the protective effects of **1** are due to either GPx-like catalysis, metal binding, or both, various cell-based assays were performed, and, where appropriate, the results obtained for **1** were compared to the ones for ebselen, tacn or DFO as representatives of catalytic and metal binding activity, respectively.

The protective effect of tacn in FEK4 cells against UVA radiation, as measured in the MTT assay, was smaller compared to the one of **1**: While **1** provided virtual complete protection (39% absolute increase in cell viability), tacn only partially protected the cells (15% increase in

viability). These results point towards a significant, yet not exclusive share of the Se moiety in the protective effect of **1**.

This initial notion was supported by an investigation of the adenosine triphosphate (ATP) levels in cells exposed to 500 kJ m⁻² UVA radiation.¹⁴ While ATP levels in cells without protection dropped by 90% upon radiation, they remained at 62% of the control value in the presence of 50 μM of **1**. DFO (at 100 μM) showed a similar protection, keeping ATP levels at 58% of the control. At 50 μM, **1** also led to a 2.2-fold increase in GPx-like activity measured in FEK4 cells. Although this effect was considerably less than the one observed for ebselen (4.0-fold increase at 5 μM), it confirmed that **1** can contribute to the catalytic antioxidant activity in the cell, albeit at a modest level - which is in accordance with the results obtained in the PhSH and MT assay.

In summary, **1** provided strong protection of FEK4 cells against 500 kJ m⁻² UVA radiation at concentrations not toxic to these cells and by a mechanism probably combining elements of metal binding (like DFO) and modest GPx-like catalysis (like ebselen).

DISCUSSION

The results obtained in this study support the notion that multifunctional compounds combining selenium and metal binding (here: macrocycle) chemistry may act as rather effective antioxidants against the oxidative damage induced by UVA radiation. Since the most promising compound, **1**, also has low toxicity in the cells tested, i.e., can be used in reasonable concentrations, this finding is interesting in itself and may be used for the future development of antioxidants in the area of skin protection, for instance in sunscreens.

This study has also provided a number of in vitro and cell culture results, which are worth considering in more detail. First of all, the catalytic and metal binding properties associated with **1** in vitro and in FEK4 cells are somewhat surprising. Rather than providing high catalytic activity, **1** is only modestly active in the PhSH and MT assays, which is also reflected in cell culture, where GPx-like activity is only increased 2.2-fold. Although this can be explained mechanistically by considering the catalytic cycle (Figure 8), it is surprising from a biochemist's point-of-view: Apparently, high catalytic activity alone does not equate the perfect antioxidant. This notion is supported by the fact that some excellent GPx-like catalysts are actually cytotoxic in the presence of H₂O₂, probably due to random use of intracellular thiol substrates.¹⁵⁻¹⁹ In contrast, more modest catalysts may behave less aggressively in cells, yet may still provide some additional GPx-like activity to protect the cells.

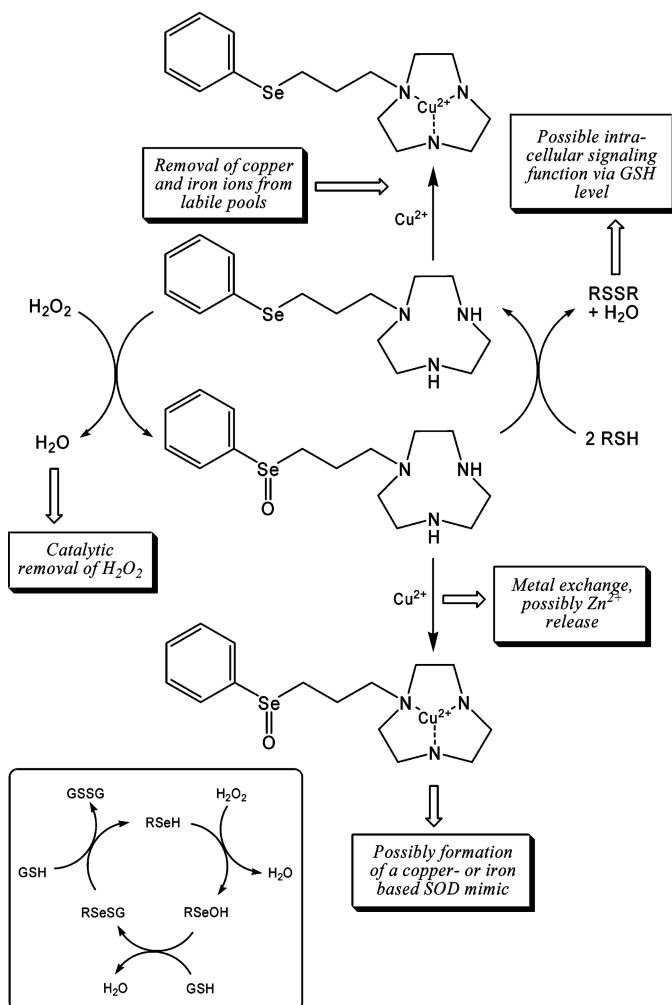


FIGURE 8 Chemical basis of protective and regulatory effects associated with **1** in cell culture. The Se-based redox center is able to catalytically remove H_2O_2 in the presence of a thiol, most likely GSH. At the same time, the tacn site is able to interact with metal ions, such as copper and iron (possibly exchanging these metal ions for others, such as zinc). In addition to these events, GPx-like catalysis and metal binding may also trigger intracellular redox signaling (e.g., via changes in GSH and GSSG levels), yield a copper- or iron-based SOD mimic (most likely for **3**) and provide an antioxidant response via zinc release. *Please note:* The image of the copper-complex is for illustration only. Copper is likely to bind to additional ligands, including H_2O , Cl^- or a second tacn molecule to achieve tetra- or hexa-coordination. The precise stoichiometry of metal binding in vivo has not yet been studied; it will depend on a number of factors and may ultimately vary.^{6,7}

A similar notion applies to metal binding. Extraordinarily strong metal chelating agents are known to be toxic in cells due to their ability to remove metal ions from proteins and enzymes. In contrast, modest metal binding agents provide protection against labile metal ions without 'freeloading' on protein bound metal ions.²⁰ As such, tacn provides some protection against UVA induced OS which is almost certainly due to sequestration of copper and/or iron ions. This effect is significantly enhanced, however, in the presence of the Se-moiety in **1**. In short, the combination of modest catalysis with modest metal binding provides good protection, while stronger agents may ultimately turn out to be toxic to the cell.

One of the aims of this study was the design and synthesis of chemically simple, yet biochemically quite active agents. The design of compounds was guided by the biochemical principle of catalytic H_2O_2 removal on the one hand and sequestration of labile copper (and iron) ions to counteract Fenton-type events on the other. The synthesis of the resulting compounds **1–3** could be carried out in a few steps and by using comparatively simple chemical procedures, albeit in comparably low yield. The latter was due to inherent problems associated with Se chemistry, the requirement for highly purified samples, and the initial lack of optimization of the synthetic method, which will be performed as part of a follow-up study.

A second aim of the study was a comparison of mono- with diselenides, such as the compounds evaluated by us previously (Figure 2). The switch from diselenides to monoselenides results in a rather different redox chemistry (Figure 8), which manifests itself in a range of in vitro findings. Diselenides are reduced to selenol(ate) by reversible two-electron transfer, which generally occurs at mercury (or other metal) electrodes around -700 to -800 mV vs. SSE. In contrast, monoselenides are irreversibly oxidized by one-electron transfer at around $+800$ to $+1200$ mV, depending on the nature of substituents attached to the Se atom.^{11,21} In this context, **1** and **2** show an oxidation behavior typical of Se oxidation, but with rather high E_{pa} values. This value is generally lower for diarylselenides, whereby the aromatic system endows Se with a lower E_{pa} value and the compound with increased chemical and metabolic stability. Future addition of more aromatic groups may therefore lower the E_{pa} value of compounds such as **1** and **2** and increase their activity. On the other hand, such aromatic systems tend to decrease solubility in water, which may ultimately be counter-productive.

Together with the redox cycle characteristic for monoselenides, the E_{pa} values of **1** and **2** may also explain their lower activity in the PhSH and MT assays when compared to the diselenides shown in Figure 2.⁵ To

counter-balance this loss of GPx-like activity, metal binding is enhanced in **1–3** by the presence of macrocyclic moieties. The electrochemical studies in the presence of Cu^{2+} and Fe^{2+} show that **1** and **2** have pronounced effects on the oxidation and reduction of these transition metal ions *in vitro*. The changes observed are similar to the ones seen for DFO, implying that **1** and **2** can remove labile copper and iron ions from their respective pools. Complexation of these metal ions is essential for the antioxidant activity of DFO.²² It also explains the protective properties of tacn shown in Figure 7 and seems to contribute to the activity of **1** in FEK4 cells.

Interestingly, our *in vitro* findings also translate into cell culture. The 2.2-fold increase in GPx-like activity in FEK4 cells, for instance, is likely to be directly due to the catalytic activity of **1**, although a more complex chain of events, such as Se-cysteine synthesis and GPx production stimulated by **1** cannot be ruled out completely at this stage. Similarly, the protection exerted by **1** against UVA-radiation, which is comparable to DFO, yet superior to tacn, points towards a combination of GPx-like catalysis and metal binding as the most likely mode(s) of protective, antioxidant action.

It is also interesting to note that a recent study has employed copper-containing tacn derivatives as antioxidants with an apparent SOD-like activity.⁶ A metal-free (or zinc-containing) tacn derivative may therefore not only act as metal sequestering agent, but also as a “smart” precursor of a metal complex, which is formed in the presence of labile copper ions and then provides antioxidant SOD-like activity. Compound **1** may therefore provide a lead structure for the development of further multifunctional antioxidants, not least because it also has shown low toxicity in cell culture.

Future studies may well expand the synthetic aspects of this work to include more complicated chemical structures, which are, in principle, possible. For instance, Singh and colleagues have recently synthesized larger Se-containing macrocycles, which provide an additional motif for the design of multifunctional antioxidants.²³ Similarly, the synthesis of protoporphyrin based Se-compounds needs to be expanded. Although our first attempts to assess these compounds *in vitro* have been marred by solubility problems, concentrations required *in vivo* are considerably lower than the ones required in our *in vitro* assays. Ultimately, more soluble derivatives of **3** may possess several advantages. They are easy to synthesize, are based on a natural moiety, contain two Se centers, strongly interact with copper and iron ions, provide the basis for a biochemically advantageous copper/iron for zinc metal exchange and may form useful SOD mimics upon copper/iron uptake (see above).

The basic metal exchange experiments, albeit providing only very rough and qualitative estimates, also bode well: It may be possible to use macrocyclic compounds to exchange labile copper and iron ions for labile zinc ions, with dramatic and highly beneficial effects on the intracellular redox environment. Furthermore, protoporphyrin compounds are likely to feature promising transport properties due to their amphiphilic character and may act as photosensitizers in the metal-free form.²³ These aspects are currently under investigation.

In conclusion, we have obtained a first set of initial, promising results using a combination of Se-based catalysis and macrocycle-based metal interactions. This approach now clearly leads itself to further, more extensive studies combining advanced synthetic chemistry with comprehensive, in depth biochemical and cell culture studies.

EXPERIMENTAL

Materials

Chemical reagents were purchased from Sigma-Aldrich-Fluka (Darmstadt, Germany) and used without further purification unless stated otherwise. 3-(N-morpholino)propanesulfonic acid (MOPS, 99%) was obtained from ACROS (Geel, Belgium) and Annexin V from Roche (Lewes, UK). Cell culture materials were from Life Technologies (Paisley, Scotland) except fetal calf serum (FCS), which was obtained from PAA Laboratories (Teddington, UK) and phosphate buffered saline (PBS), which was from Oxoid (Basingstoke, UK). Apoglow kit reagents were from Lumintech (Nottingham, UK). Cd,Zn-MT was purchased from Sigma and Zn₇-MT was reconstituted and purified according to a standard method.²⁴ Deionised, MilliQ water (resistance ≥ 18 M Ω cm) was used for the electrochemical, in vitro and cell culture experiments.

For chemical synthesis, dry solvents were essential for the synthesis of compounds, i.e., acetonitrile, THF and CH₂Cl₂ were refluxed with calcium hydride and freshly distilled before use. Dry DMF was purchased from Fluka. All reactions were carried out under Argon (4.6) using standard Schlenk techniques. Silica gel (Macherey-Nagel, 50–200 μ m) was used for column chromatography.

¹H NMR spectra were recorded at 500 MHz, ¹³C NMR spectra at 125 MHz on a Bruker Avance 500 spectrometer. Chemical shifts are reported in δ (ppm), expressed relative to the solvent signal at 7.26 ppm (CDCl₃, ¹H NMR) and at 77.16 ppm (CDCl₃, ¹³C NMR).

For LC-MS a RP C18 NUCLEODUR[®] 100-3 (125 × 3 mm) column (Macherey-Nagel GmbH, Dueren, Germany) was used as stationary phase and MS analysis was performed on a TSQ Quantum mass spectrometer equipped with an ESI source and a triple quadrupole mass detector (Thermo Finnigan, San Jose, CA). A gradient of methanol (containing 0.1% formic acid) in water (containing 0.1% formic acid) was used, which varied from 5% to 100% over 13 min at a flow rate of 400 $\mu\text{l min}^{-1}$.

Synthesis of compounds 1–3

1-[3-(phenylseleno)propyl]-1,4,7-triazacyclononane (compound 1, Figure 3a)

1,4,7-Triazacyclononane (tacn, 137.1 mg, 1.06 mmol) was dissolved in 30 ml of dry acetonitrile and K_2CO_3 (138.2 mg, 1.0 mmol) was added at room temperature. A solution of 1-bromo-3-phenylselenopropane²⁵ (183.6 mg, 0.66 mmol) in 20 ml of dry acetonitrile was then added dropwise over 1.5 h. The reaction was kept at room temperature and stirred overnight. The solvent was then evaporated. The residue was taken up in MeOH and CH_2Cl_2 , the resulting solution was filtered and the solvent evaporated to yield the product as light yellow viscous oil (210.1 mg, 0.64 mmol) in 97.5% yield.

$\text{C}_{15}\text{H}_{25}\text{N}_3\text{Se}$ ($M_r = 326.34 \text{ g mol}^{-1}$). ¹H NMR (500 MHz, CDCl_3): $\delta = 1.81$ (quint, 2 H, $\text{CH}_2\text{CH}_2\text{CH}_2$, $^3J_{\text{HH}} = 6.9 \text{ Hz}$), 2.88 (m, 18 H, CH_2 bridge, CH_2 tacn, NH), 7.20 (m, 3 H, CH phenyl), 7.45 (m, 2 H, CH phenyl).

¹³C NMR (125 MHz, CDCl_3): $\delta = 25.2, 34.0, 42.1, 48.9, 49.2, 57.8$ (CH_2 bridge, CH_2 tacn), 126.9, 129.1, 130.4, 132.7 (CH phenyl, C_q).

LC-MS: t_R , m/z (%) = 5.7 min, 257.0 (100) [$\text{PhSeC}_3\text{H}_6\text{NC}_2\text{H}_4\text{NH}+\text{H}$]⁺, 216.0 (45) [$\text{PhSeC}_3\text{H}_6\text{NH}_2+\text{H}$]⁺.

1,7-bis[3-(phenylseleno)propyl]-1,4,7,10-tetraazacyclododecane (Compound 2, Figure 3b)

Compound 2 was synthesized by two alternative methods, one involving nucleophilic substitution on a brominated precursor, the other Schiff base formation with subsequent reduction (see Figure 3b).

The first method was analogous to the synthetic method for 1. To a solution of 1,4,7,10-tetraazacyclododecane (cyclen, 172.3 mg, 1.0 mmol) and K_2CO_3 (138.2 mg, 1.0 mmol) in dry acetonitrile was added 1-bromo-3-phenylselenopropane (139.0 mg, 0.5 mmol) dropwise at room temperature over 1.5 h. The solution was stirred at room temperature

overnight and filtered. The solvent was subsequently evaporated to yield a light yellow oil as crude product, which was purified by preparative HPLC using a gradient of 25% to 100% of methanol (containing 0.1% formic acid) in water (containing 0.1% formic acid). Retention time of product: $t_R = 20\text{--}24$ min. The solvent was then removed under reduced pressure to yield a white solid. In order to avoid formic acid salts of the product, the latter was dissolved in 30 ml CH_2Cl_2 , washed with 10 ml conc. NH_3 solution and after that with water until the pH of the washings was 7.0. The organic layer was separated and dried over Na_2SO_4 . CH_2Cl_2 was evaporated to give the desired product as lightly yellowish, highly viscous oil (42.2 mg, 0.074 mmol) in 29.8% yield.

Alternatively, cyclen (172.3 mg, 1.0 mmol) was dissolved in 25 ml of dry THF. A solution of 3-(phenylseleno)propanal²⁶ (426.3 mg, 2.0 mmol) in 18 ml was added dropwise at room temperature over a period of 10 min. After 15 min, sodium triacetoxyborohydride (593.4 mg, 2.8 mmol) was added and the reaction was stirred at room temperature overnight. The solvent was evaporated under reduced pressure and the crude product was purified by preparative HPLC as described above to give the desired product as lightly yellowish, viscous oil (73.7 mg, 0.13 mmol) in 13.0% yield.

$\text{C}_{26}\text{H}_{40}\text{N}_4\text{Se}_2$ ($M_r = 566.54 \text{ g mol}^{-1}$). $^1\text{H NMR}$ (500 MHz, CDCl_3): $\delta = 1.84$ (quint, 4 H, $\text{CH}_2\text{CH}_2\text{CH}_2$, $^3J_{\text{HH}} = 6.9$ Hz), 2.54 (m, 14 H, CH_2 tacn, CH_2 bridge, NH), 2.63 (t, 8 H, CH_2 tacn, $^3J_{\text{HH}} = 4.7$ Hz), 2.88 (t, 4 H, CH_2 bridge, $^3J_{\text{HH}} = 6.9$ Hz), 7.22 (m, 6 H, CH phenyl), 7.46 (m, 4 H, CH phenyl).

$^{13}\text{C NMR}$ (125 MHz, CDCl_3): $\delta = 25.8, 27.4, 45.6, 52.2, 54.7$ (CH_2 bridge, CH_2 cyclen), 126.7, 129.1, 130.6, 132.6 (CH phenyl, C_q).

LC-MS: t_R , m/z (%) = 7.2 min, 569.1 (100) $[\text{M}+\text{H}]^+$.

3,3'-(3,7,12,17-Tetramethyl-8,13-divinylporphyrin-2,18-diyl)bis{N-[3-(phenylseleno)propyl]propanamide} (Compound 3, Figure 3c)

Compound **3** was synthesized from protoporphyrin IX and an appropriate selenium precursor, 3-(phenylseleno)propan-1-amine, by two alternative methods, one involving the acid chloride reaction with amine, the other a coupling of the acid with amine using ethylchloroformate (Figure 3c).

As part of the first method, a suspension of protoporphyrin IX disodium salt (106.0 mg, 0.18 mmol) in 10 ml dry CH_2Cl_2 was treated with a large excess oxalylchloride (CO_2Cl_2 , 1 ml). The resulting green suspension was stirred at room temperature in the dark for 2 h. The solvent and excess CO_2Cl_2 were removed under reduced pressure and

the residue containing crude protoporphyrin bis(acid)chloride was re-dissolved in 15 ml CH_2Cl_2 and used without further purification. It was added dropwise to a solution of 3-(phenylseleno)propan-1-amine^{27,28} (275.0 mg, 1.28 mmol) and triethylamine (4 ml) in 55 ml dry DMF over 30 min. The reaction was then stirred at room temperature overnight. The solvent was removed under reduced pressure and the resulting brown residue was dissolved in 50 ml of CH_2Cl_2 and washed three times with saturated brine. The organic layer was dried over Na_2SO_4 , filtered and the solvent removed under reduced pressure to give a dark black solid. The impure product was cleaned by three consecutive silica gel column chromatography purifications, using solvents CH_2Cl_2 and MeOH (95:5). The product, **3**, was obtained as a purple solid (25.6 mg, 0.03 mmol) in a yield of 16.7%.

$\text{C}_{52}\text{H}_{56}\text{N}_6\text{O}_2\text{Se}_2$ ($M_r = 954.96 \text{ g mol}^{-1}$). $^1\text{H NMR}$ (500 MHz, CDCl_3): $\delta = 1.38\text{--}1.47$ (m, 4 H, CH_2), 2.19–2.22, 2.24–2.27 (each t, 2 H, CH_2 , $^3J_{\text{HH}} = 7.0 \text{ Hz}$), 2.92–2.96 (t, 4 H, CH_2 , $^3J_{\text{HH}} = 7.6 \text{ Hz}$) 2.98–3.05 (m, 4 H, COCH_2), 3.37, 3.40, 3.45, 3.55 (each s, 3 H, CH_3), 4.16–4.20 (m, 4 H, COCH_2CH_2), 6.06–6.15, 6.20–6.31 (each m, 2 H, CH_2 vinyl), 6.74, 6.82 (each s, 1 H, CONH), 6.95–7.06 (m, 8 H, CH phenyl), 7.52–7.54, 7.70–7.72 (each m, 1 H, CH phenyl), 7.97–8.03, 8.11–8.17 (each m, 1 H, CH vinyl), 9.71, 9.76, 9.79, 9.86 (each s, 1 H, CH methin).

LC-MS: t_R , m/z (%) = 15.7 min, 957.2 (100) $[\text{M}+\text{H}]^+$.

The comparably low yield of the acid chloride to amine coupling may have been due to the rather aggressive chemicals used. As an alternative, coupling with ethylchloroformate was investigated. Protoporphyrin IX (111.4 mg, 0.20 mmol) was dissolved in 5 ml dry chloroform and cooled to 0°C . N-methylmorpholine (45.9 mg, 0.45 mmol) was added and the mixture was stirred at 0°C for 15 min. Ethylchloroformate (52.4 mg, 0.48 mmol) was added and the reaction mixture was stirred at 0°C for another 30 min. At this point, 3-(phenylseleno)propane-1-amine (99.8 mg, 0.47 mmol) was added and the reaction was stirred at 0°C for 1 h, followed by stirring at room temperature overnight. The solvent was removed under reduced pressure and the resulting brown residue was purified once by column chromatography as described above, to obtain **3** as a purple metallic solid (117.6 mg, 0.12 mmol) in a yield of 62.1%. Analytical data was in accordance with the one obtained by the CO_2Cl_2 coupling method.

Electrochemistry

Cyclic Voltammograms were recorded at a BAS 100W electrochemical workstation to evaluate the redox behavior of the Se-compounds and

their interactions with Cu^{2+} ions. In all electrochemical experiments, recordings were taken on a glassy carbon working electrode (which was cleaned with Al_2O_3 and H_2O between each recording), using an Ag/AgCl electrode (SSE) as reference and a platinum spiral as counter electrode. Unless stated otherwise, Cyclic Voltammograms were recorded at 20°C with a scan rate of 500 mV s^{-1} . Three full cycles were recorded as part of each scan, and all experiments were performed in triplicate. Ferrocene was used as a reference to control/adjust the potential scale.

Oxidation of the Se-redox center was studied between -500 mV and $+1300\text{ mV}$ vs. SSE in potassium phosphate (KPi) buffer (pH 7.4), containing 33% methanol to ensure sufficient solubility of the compounds tested. In accordance with our previous studies, the interaction with Cu^{2+} ions was studied in 10 mM MOPS buffer (pH 7.4) to avoid precipitation of metals/ligand or significant metal-buffer interactions.⁵ The buffer was treated with Chelex 100 prior to use to remove any traces of interfering metal ions. The potential range was between -350 mV and $+550\text{ mV}$ vs. SSE.

UV/VIS Spectrophotometry and UV-Based Assays for Catalytic Activity

UV/VIS spectra were recorded on a Cary 50 Bio spectrophotometer from Varian Inc.. Unless stated otherwise, quartz cuvettes were used throughout. All recordings were taken at 20°C and repeated at least three times.

The thiophenol (PhSH) assay, which is indicative of catalysts enhancing the rate of reaction of H_2O_2 with PhSH, was employed to assess the catalytic activity of compounds. This assay is somewhat easier to use when compared to the coupled GPx-assays or the MT assay. It avoids solubility problems often associated with aromatic Se-compounds by operating in methanol and provides a fast and reliable method for assessing (catalyzed) thiol oxidation events. In short, thiophenol (1 mM final concentration) was dissolved in methanol and oxidation of the thiol was initiated by addition of 2 mM H_2O_2 . The formation of PhSSPh was followed at 305 nm and 20°C for 60 min and the initial rates of reaction (1 to 10 min) were compared for reactions in the absence and presence of Se-compounds (100 μM each).⁵ Ebselen was used as a positive control.

The more complicated MT assay, which measures the oxidative release of Zn^{2+} ions from the zinc/sulfur protein MT and subsequent uptake of the metal ion by the chromophoric dye 4-(2-pyridylazo)-resorcinol (PAR), was used for the most promising compound, **1**.²⁹

The experimental procedure was identical to the one described in the literature.

FEK4 Cell Culture

The human skin fibroblast cells FEK4 and FCP7 were derived from newborn foreskin explants.^{13,14} Cells were cultured routinely in Earle's minimal essential medium (EMEM) supplemented with 2 mM L-glutamine, 50 u/ml penicillin, 50 μ g/ml streptomycin, 0.2% sodium bicarbonate and 15% FCS and incubated in a humidified atmosphere at 37°C with 5% CO₂. For experiments, fibroblast monolayers were grown in dishes/coverslips for 3–4 days in order to reach 80% confluency. FEK4 cells were used between passages 12 to 14 and FCP7 cells between passages 4 to 11.

Selenium compounds were dissolved in DMSO and added to the cell medium at the required concentrations 18 h prior to experiments. The concentration of DMSO was kept constant at 0.1% of the medium in order to avoid cellular effects of the vehicle itself. Control cells were pretreated with DMSO alone.

For the irradiation step, the medium was removed from the cells and retained as a condition medium. Cells were washed with PBS and covered in 2 ml of warm PBS containing Ca²⁺ and Mg²⁺ ions (0.01% CaCl₂ and MgCl₂). Monolayers of cells were irradiated at 25°C using a broad spectrum Sellas 4kW UVA lamp (Sellas, Germany) with significant emission in the range of 350–400 nm. UVA doses were measured using an IL1700 radiometer (International Light, Newburyport, MA). The UVA doses used were 250 kJ m⁻² (moderate dose) and 500 kJ m⁻² (high dose), which are equivalent to the amount the surface of the skin would be exposed to over 70 or 140 min, respectively, at noon on a cloudless summer day, at a northern latitude of 30 to 35°.

After irradiation, cells were washed with PBS, the condition medium was added back and cells were incubated at 37°C for 4 h. Control cells were treated in the same manner, except that they were not irradiated and were instead stored in dark conditions at room temperature during the irradiation process. Cell viability was measured with the MTT colorimetric assay at 550 nm using a MR5000 microplate reader (Dynatech Laboratories, West Sussex, UK).

The GPx activity in FEK4 cells was measured according to the method by Flohé and Gunzler, whereby NADPH consumption at 340 nm is used as a measure of the rate of glutathione disulfide (GSSG) formation due to the GPx reaction (the assay is initiated by the addition of GSH, ^tBuOOH and NADPH).³⁰ ATP was measured using the commercially available Apoglow adenylate nucleotide ratio assay.¹⁴

REFERENCES AND NOTES

- [1] B. Halliwell and J. M. C. Gutteridge, *Free Radicals in Biology and Medicine*, 4th ed. (Oxford University Press, Oxford, 2007).
- [2] Z. A. Wood, E. Schroder, J.R. Harris, and L.B. Poole, *TIBS*, **28**, 32–40 (2003).
- [3] Many of these catalysts do, of course, require a reductant as co-substrate to function, with the notable exception of SOD and CAT which redox-disproportionate $\text{O}_2^{\bullet-}$ and H_2O_2 , respectively. In the case of GPx and Prx, GSH and reduced thioredoxin (Trx) act as respective co-substrates. While this dependency may be seen as a potential disadvantage, it also provides a certain element of biochemical feedback and control: Once GSH or Trx levels are depleted in the cell, these antioxidant enzymes switch off, the cellular defense capitulates and the cell undergoes (controlled) cell death. This chain of events has recently been studied to considerable extent for the Prx enzymes.
- [4] G. Mugesch and H. B. Singh, *Chem. Soc. Rev.*, **29**, 347–357 (2000).
- [5] C. A. Collins, F. H. Fry, A. L. Holme, A. Yiakouvaki, A. Al-Qenaei, C. Pourzand, and C. Jacob, *Org. Biomol. Chem.*, **3**, 1541–1546 (2005).
- [6] Q. X. Li, Q. H. Luo, Y. Z. Li, and M. C. Shen, *Dalton Trans.*, 2329–2335 (2004).
- [7] X. Liang and P. J. Sadler, *Chem. Soc. Rev.*, **33**, 246–266 (2004).
- [8] K. Pong, *Expert. Opin. Biol. Ther.*, **3**, 127–139 (2003).
- [9] The oxidation wave of Fe^{2+} was not clearly observable due to low concentrations of the metal ion in solution, which in turn was limited by the solubility of **1** and **2**.
- [10] Changes in the UV region between 260 nm and 360 nm are not due to metal binding to protoporphyrin but are associated with the copper and iron ions themselves.
- [11] G. I. Giles, F. H. Fry, K. M. Tasker, A. L. Holme, C. Peers, K. N. Green, L. O. Klotz, H. Sies, and C. Jacob, *Org. Biomol. Chem.*, **1**, 4317–4322 (2003).
- [12] Compound **3** was poorly soluble in aqueous media and no identifiable oxidation current could be observed.
- [13] C. Pourzand, R. D. Watkin, J. E. Brown, and R. M. Tyrrell, *Proc. Natl. Acad. Sci. USA*, **96**, 6751–6756 (1999).
- [14] J. L. Zhong, A. Yiakouvaki, P. Holley, R. M. Tyrrell, and C. Pourzand, *J. Invest. Dermatol.*, **123**, 771–780 (2004).
- [15] N. M. Giles, N. J. Gutowski, G. I. Giles, and C. Jacob, *FEBS Lett.*, **535**, 179–182 (2003).
- [16] N. M. Giles, G. I. Giles, J. E. Holley, N. J. Gutowski, and C. Jacob, *Biochem. Pharmacol.*, **66**, 2021–2028 (2003).
- [17] G. I. Giles, N. M. Giles, C. A. Collins, K. Holt, F. H. Fry, P. A. S. Lowden, N. J. Gutowski and C. Jacob, *Chem. Commun.*, 2030–2031 (2003).
- [18] F. H. Fry, A. L. Holme, N. M. Giles, G. I. Giles, C. Collins, K. Holt, S. Pariagh, T. Gelbrich, M. B. Hursthouse, N. J. Gutowski, and C. Jacob, *Org. Biomol. Chem.*, **3**, 2579–2587 (2005).
- [19] F. H. Fry and C. Jacob, *Current Pharm. Des.*, **12**, 4479–4499 (2006).
- [20] Z. D. Liu and R. C. Hider, *Coord. Chem. Rev.*, **232**, 151–171 (2002).
- [21] G. I. Giles, K. M. Tasker, R. J. K. Johnson, C. Jacob, C. Peers, and K. N. Green, *Chem. Commun.*, 2490–2491 (2001).
- [22] G. S. Tilbrook and R. C. Hider, *Metal Ions in Biological Systems*, **35**, 691–730 (1998).
- [23] S. Panda, S. S. Zade, H. B. Singh, and R. J. Butcher, *Eur. J. Inorg. Chem.*, 172–184 (2006).
- [24] M. Vařák, *Methods Enzymol.*, **205**, 41–44 (1991).
- [25] J. E. Baldwin, R. M. Adlington, and J. Robertson, *Tetrahedron*, **45**, 909–922 (1989).

- [26] S. Harusawa, S. Tomii, C. Takehisa, H. Ohishi, R. Yoneda, and T. Kurihara, *Chem. Pharm. Bull.*, **40**, 2279–2282 (1992).
- [27] A. Khanna, A. Bala, and B. L. Khandelwal, *J. Organomet. Chem.*, **494**, 199–204 (1995).
- [28] S. V. Amosova, N. A. Makhaeva, A. V. Martynov, V. A. Potapov, B. R. Steele, and I. D. Kostas, *Synthesis*, 1641–1648 (2005).
- [29] C. Jacob, W. Maret, and B. L. Vallee, *Proc. Natl. Acad. Sci. U. S. A.*, **96**, 1910–1914 (1999).
- [30] L. Flohe and W. A. Gunzler, *Methods Enzymol.*, **105**, 114–121 (1984).
- [31] E. O. Hileman, J. Liu, M. Albitar, M. J. Keating, and P. Huang, *Cancer Chemother Pharmacol*, **53**, 209–219 (2004).